

Appendix B from D. A. Kennedy et al., “Pathogen Growth in Insect Hosts: Inferring the Importance of Different Mechanisms Using Stochastic Models and Response-Time Data”

(Am. Nat., vol. 184, no. 3, p. 407)

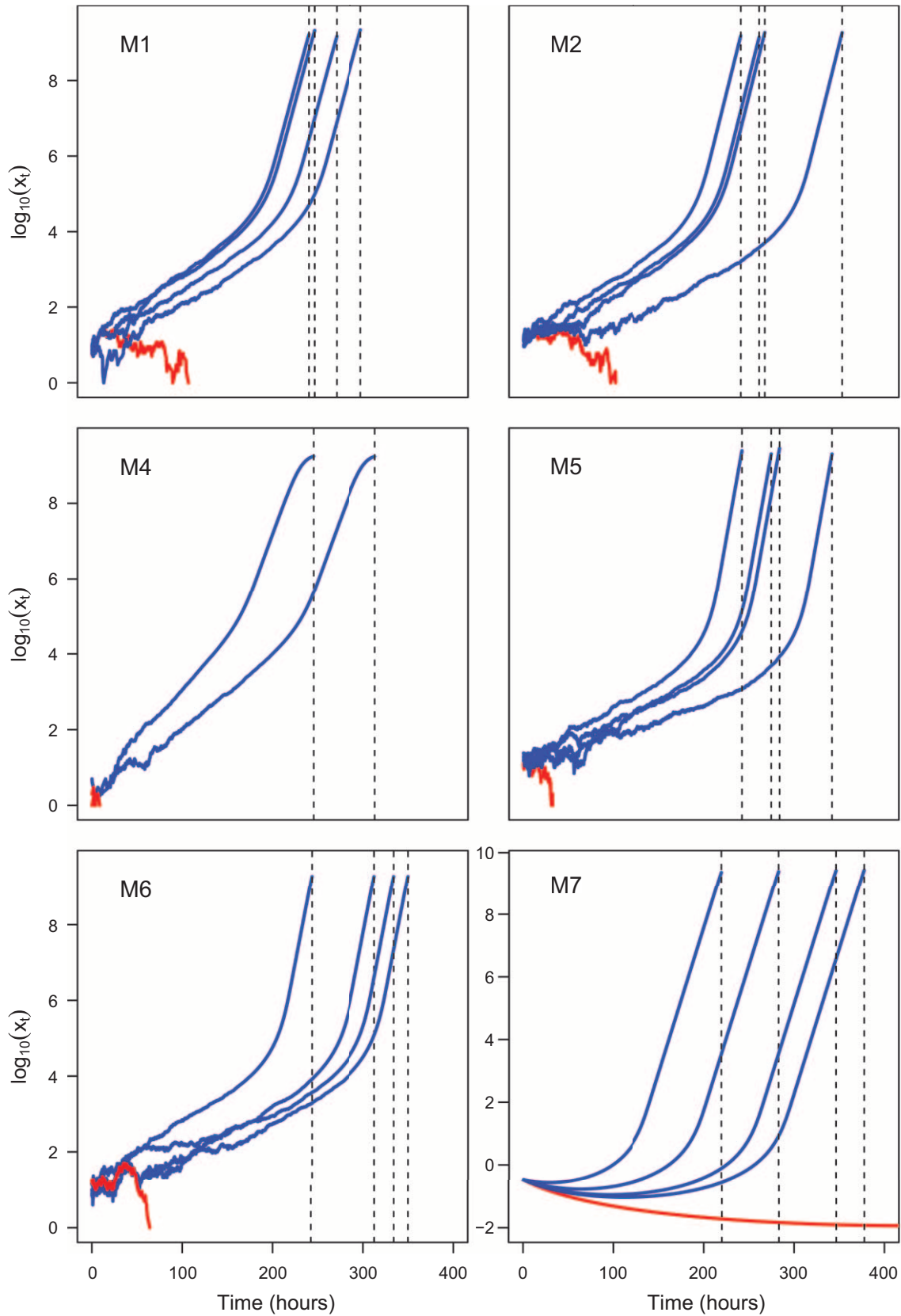


Figure B1: Realizations of six of the seven models in the main text (M1: most complex model, M2: linear virus growth, M4: linear virus

colonization, M5: identical immune system, M6: identical response threshold, and M7: no demographic stochasticity). Each panel shows five stochastic realizations generated using a hybrid simulation (except for the no-demographic-stochasticity model M7, which was generated using only the Euler method). The hybrid simulation algorithm used the Gillespie method to exactly simulate a trajectory until the virus population size reached 10^4 , at which time demographic stochasticity becomes negligible, and the remainder of the trajectory can be closely approximated by numerical integration of the corresponding ordinary differential equation model. Numerical integration was carried out using the Euler method. In each case, we used the parameter set from our Markov chain Monte Carlo chains with the highest joint posterior probability for the model under consideration. Blue trajectories show realizations in which the virus causes host death, while red trajectories show realizations in which the host survives. Simulations were chosen to illustrate cases in which some individuals died and some survived, to illustrate what the model trajectories look like in each case. Note that in the no-demographic-stochasticity model (M7), the initial number of virus particles is slightly less than 1. This feature of model M7 arises because the model assumes that the virus population can be approximated as a continuous variable. The Shortley birth-death model (M3) is not included, because generating even a single realization of that model using the maximum posterior parameter set would have required weeks of computing time. We instead refer the reader to figure 2 to visualize the behavior of that model.

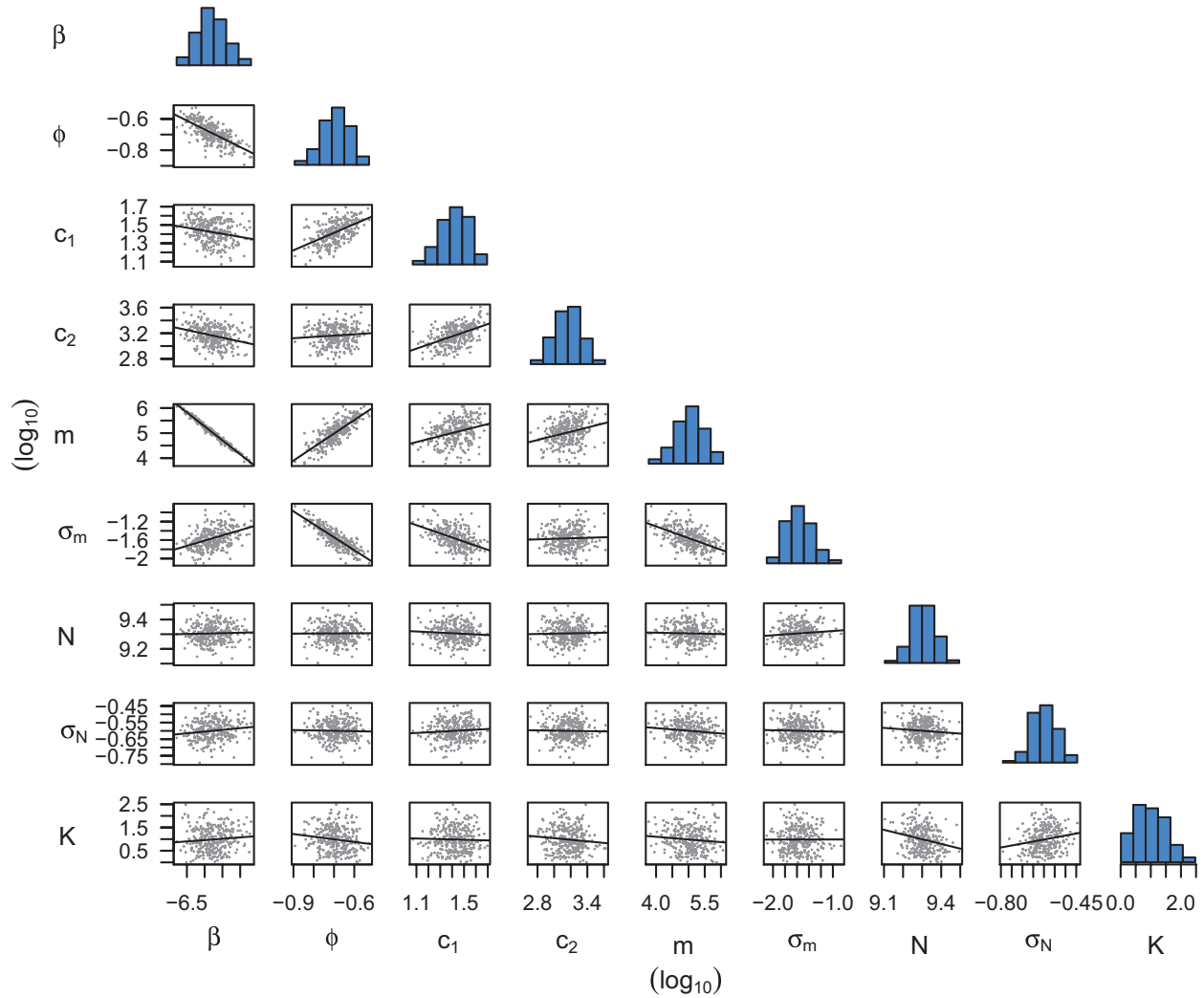


Figure B2: Pairwise parameter correlations. Three hundred parameter sets were sampled without replacement from the posterior distribution of our most complex model (M1). Histogram plots show the marginal distribution for the respective resampled parameters, and dot plots show the pairwise correlation. Best-fit lines show that some parameter combinations are strongly correlated while others are not.